

A Safety-focused Vehicle Driving Strategy Towards Minimal Injury Severity In Imminent Collision Scenarios

Qingfan Wang, Wentao Chen, Zhiwei Sun, Miao Lin, Qing Zhou, Bingbing Nie*

I. INTRODUCTION

Road traffic accidents remain a worldwide public health concern. Reducing the occurrence rate and mitigating the injury severity of motor vehicle crashes are two major topics in the road traffic safety field. On the one hand, the recent development of highly automated vehicles (HAVs) is expected to improve traffic safety by avoiding potential collisions in hazardous conditions, categorised as active safety [1]. On the other hand, passive safety, such as vehicle body structure and occupant constraint design, significantly mitigates occupant injuries in road traffic accidents [2]. However, existing active and passive occupant protection systems are usually developed separately, failing to make the most use of the critical time window prior to a collision. This study aims to propose an occupant safety-focused vehicle driving strategy for minimal injury severity in imminent collision scenarios by integrating injury prediction into vehicle trajectory planning for application in the next generation of safer HAVs.

II. METHODS

The framework of the safety-focused driving strategy is shown in Fig. 1. When on-vehicle sensors perceive an unavoidable obstacle, the HAV immediately estimates the collision condition and predicts the corresponding occupant injury severity in real-time. The optimal strategy is then solved under a rolling optimization method, with a discretized strategy space defined via vehicle dynamics model. We estimated the effectiveness of the whole framework in injury mitigation by reconstructing real-world collision accidents.

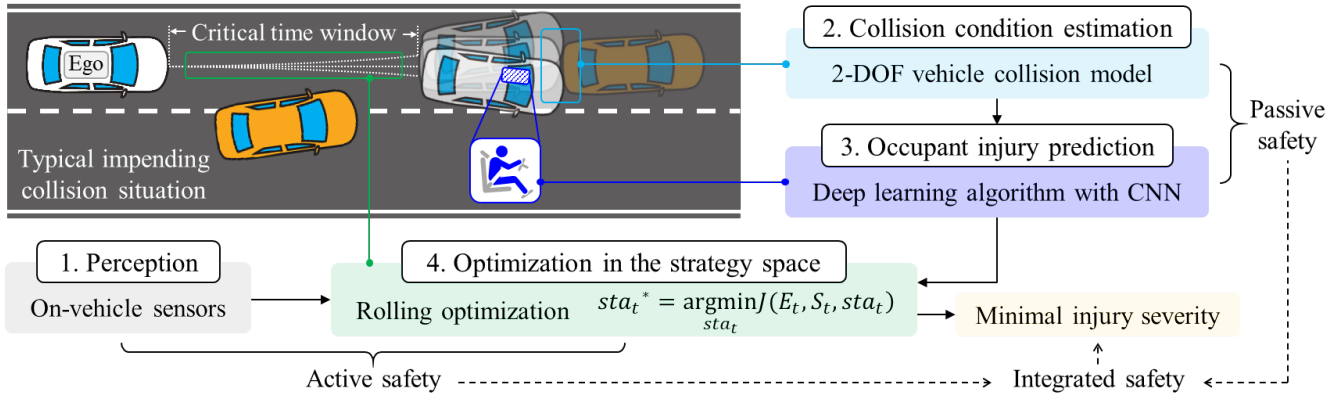


Fig. 1. The framework of the safety-focused strategy for minimal injury risk in impending collision situations.

Occupant injury prediction

Δv prediction We first estimated Δv before the collision given its strong correlation with occupant injury severity (Eq. 1). The collision severity estimation is based on the plane 2-DOF rigid-body collision model with momentum conservation (Fig. 2(a)) [3].

$$P = \frac{(1+e)(v_2^n + h_2 w_2 - v_1^n - h_1 w_1)}{1/m_1 + 1/m_2 + h_1^2/I_1 + h_2^2/I_2}, \quad e = \frac{C}{v_2^n + h_2 w_2 - v_1^n - h_1 w_1}, \quad \Delta v_1 = \frac{P}{m_1}, \quad \Delta v_2 = \frac{P}{m_2} \quad (1)$$

where P denotes the collision impulse; e is the vehicle restitution coefficient; Coefficient C depends on the principal impact direction in traffic accident reconstruction [3]. For the two vehicles in a collision (i.e. $i = 1$ and 2), v_i^n indicates the velocity component in the impulse direction; m_i , I_i , w_i and h_i denote the mass, the moment of inertia, the yaw rate, and the distance from CG to the impulse line, respectively.

B. Nie (e-mail: nbb@tsinghua.edu.cn; tel: +86-10-6278-8689) is an Associate Professor, Q. Wang, W. Chen and Z. Sun are PhD students and Q. Zhou is a Professor, all in the School of Vehicle and Mobility at Tsinghua University. M. Lin is Head of the Traffic Accident Research Department at China Automotive Technology & Research Center (CATARC), Tianjin, China.

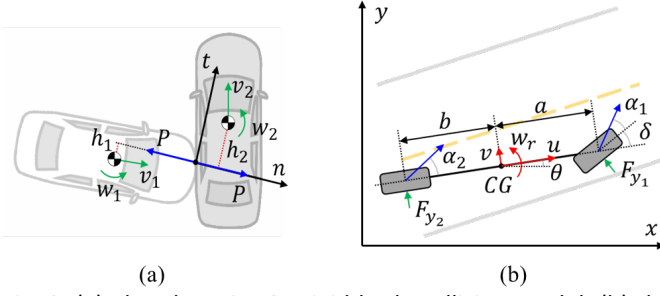


Fig. 2. (a) The plane 2-DOF rigid-body collision model; (b) the plane vehicle bicycle model.

Optimization level	Controllable objects	Availability of V2VCs
EUS	Ego vehicle	Unavailable
EAS	Ego vehicle	Available
MUS	All vehicles	Unavailable
MAS	All vehicles	Available

Injury prediction With the recent progress in data-driven methods, deep learning algorithms have been integrated into occupant injury prediction and have demonstrated satisfying performance [4]. We established a convolutional neural network (CNN) developed in a previous study using a numerical driver injury dataset [5]. The CNN can predict the time histories of drivers' kinetic responses from pre-crash information (Fig. 3). The kinetics were then translated into injury severity (i.e. abbreviated injury scale, AIS) based on the injury risk criteria. The CNN-based algorithm was validated in a real-world accident dataset from NASS/CDS and achieved a prediction accuracy of 78.7%, 95.6%, 90.2% for head, chest and neck AIS, respectively. The prediction was accomplished in near real-time. The mean probability of suffering head, chest and neck injury $P(AIS_{2+})$ was used to assess the driver's injury severity.

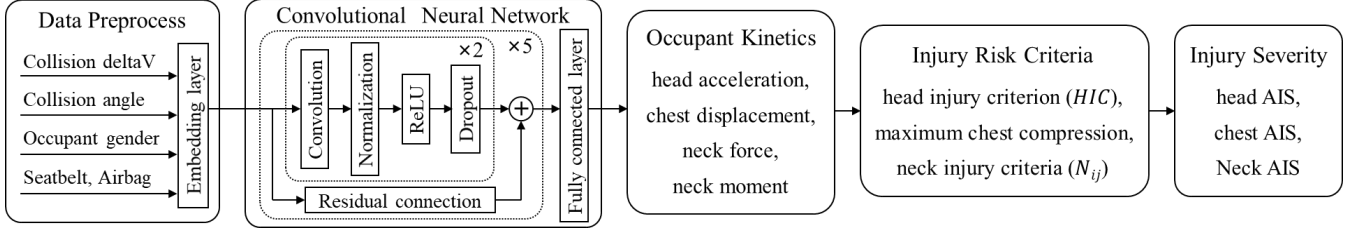


Fig. 3. The CNN-based driver injury prediction algorithm.

Vehicle dynamics and strategies

Dynamics modelling The vehicle dynamics were modelled by the widely used plane bicycle model (Eq. 2 and Eq. 3) (Fig. 2(b)). Considering that the vehicle dynamics usually dramatically change in impending collision situations, the vehicle tyre model with saturation was utilized to model the lateral tyre forces (Eq. 4):

$$\sum F_y = m(\dot{v} + uw_r) = F_{y_1} \cos \delta + F_{y_2}, \quad \sum M_z = I_z \dot{w}_r = aF_{y_1} \cos \delta - bF_{y_2} \quad (2)$$

$$x = u \cos \theta - v \sin \theta, \quad y = v \cos \theta + u \sin \theta, \quad \dot{\theta} = w_r \quad (3)$$

$$F_{y_1} = \begin{cases} -C_{\alpha_1} \alpha_1, & \text{if } \alpha_1 < \bar{\alpha}_1 \\ \bar{F}_{y_1}, & \text{if } \alpha_1 \geq \bar{\alpha}_1 \end{cases}, \quad F_{y_2} = \begin{cases} -C_{\alpha_2} \alpha_2, & \text{if } \alpha_2 < \bar{\alpha}_2 \\ \bar{F}_{y_2}, & \text{if } \alpha_2 \geq \bar{\alpha}_2 \end{cases}, \quad \alpha_1 = \beta + \frac{aw_r}{u} - \delta, \quad \alpha_2 = \beta - \frac{bw_r}{u} \quad (4)$$

where m denotes the vehicle mass; I_z is the vehicle moment of inertia; a , b are the distances from the centre of gravity (CG) to the rear or front axles; u , v are the vehicle longitudinal or lateral velocities; w_r is the yaw rate; x , y are the vehicle longitudinal or lateral positions; θ denotes the vehicle heading angle; δ is the front steering angle; $\beta = \arctan(v/u)$ is the sideslip angle of CG. For the vehicle tyres (i.e. $j = 1$ and 2 for the front and rear tyres, respectively), F_{y_j} , \bar{F}_{y_j} , α_j , $\bar{\alpha}_j$ and C_{α_j} denote the lateral force, the saturated lateral force, the tyre sideslip angle, the saturated sideslip angle and the cornering stiffness, respectively.

Discretized strategy space The vehicle driving strategy space, i.e. longitudinal acceleration and lateral swerve, is continuous in reality. To balance the optimization and computational efficiency, we discretized the solving space into 25 strategies, comprised of five acceleration strategies (acceleration, half-acceleration, constant, half-deceleration, deceleration) multiplied by five swerve strategies (left, half-left, straight, half-right, right) within the limit constraint of vehicle dynamics.

Optimized strategy

Rolling optimization The optimized driving strategy was solved under a rolling optimization method in three steps: (I) estimate the dynamics of the ego vehicle (E_t) and the surrounding vehicles (S_t) at time step t ; (II) predict

the potential collision conditions and occupant injuries $J(\cdot)$ of 25 discretized strategies (sta_t) in the strategy space, respectively, then solve the optimization problem to obtain the optimal strategy that can result in the minimum injury severity $sta_t^* = \underset{sta_t}{\operatorname{argmin}} J(E_t, S_t, sta_t)$; (III) get new measurements to update the estimation of vehicle dynamics (E_{t+1}, S_{t+1}) at time step $t + 1$ and repeat the optimization until the collision occurs.

Optimization level We defined the controllable objects as the vehicles for which driving strategies can be optimized. In addition, driving strategies of a HAV are closely related to the surrounding vehicles' dynamics, which can be directly obtained based on vehicle-to-vehicle communications (V2VCs). Considering the controllable objects and the availability of V2VCs, we defined four levels for the safety-focused strategies (Table I): ego-unavailable-level strategy (EUS); ego-available-level strategy (EAS); multi-unavailable-level strategy (MUS); multi-available-level strategy (MAS). Only MAS can converge to a globally optimal solution; the others are locally optimal. When V2VCs were not available, we used a constant-speed model to predict the surrounding vehicles' dynamics. Furthermore, autonomous emergency braking (AEB), a widely used active safety technology, was regarded as the baseline of injury mitigation. We assumed that the ego vehicle brakes immediately with the maximum deceleration when AEB is activated and that no evasive measures of swerving are allowed.

Real-world accident data

To estimate the proposed framework's effectiveness, we reconstructed 20 real-world collision cases that represented typical impending collision situations screened from the China in-depth accident study (CIDAS) database, i.e. collisions between two sedans with at least one occupant who suffered MAIS2+ injuries. Each case has detailed information involving the vehicle (e.g. mass, size), occupant (e.g. age, gender), restraint system (e.g. belt, airbag) and vehicle dynamics (1 s before and 1 s after impact). The potential reduction in injury risk in the 20 cases was calculated at different optimization levels.

III. INITIAL FINDINGS

Statistics analysis of injury mitigation

The 20 real-world accidents were reconstructed with strategies at different optimization levels. The optimized strategies and the baseline (i.e. AEB) were set to be activated at different timings covering a 1 s critical time window prior to the collision. Figure 4 compares the effectiveness of four safety-focused strategies and AEB in injury mitigation. In terms of time sensitivity, the mitigation of injury severity is positively associated with the activation time for all strategies, i.e. the earlier it intervenes, the lower the injury severity can be obtained. There are apparent differences in injury mitigation among five strategies: MAS shows the best performance (e.g. mitigating injury severity by 100% and 37.8% when activated before -500 and -300 ms, respectively). The effectiveness of MUS, EAS, EUS and AEB follows in order.

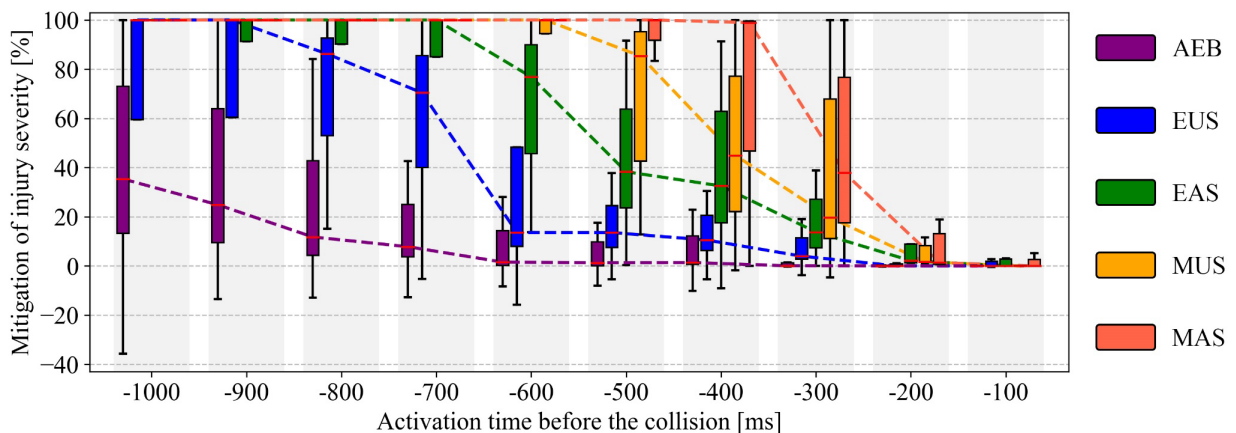


Fig. 4. Effectiveness comparison on injury severity mitigation compared with application to real-world accidents.

Case study of optimized vehicle trajectory and corresponding injury

One representative accident case is selected and analyzed in detail. Compared with Fig. 4, a similar variation trend of injury mitigation is found (Fig. 5(a)). The detailed vehicle trajectories and collision conditions demonstrate that compared with AEB and EAS, MAS successfully changes the potential impact point from the middle to the rear end of the vehicle, effectively reducing the driver's injury severity (Fig. 5(b)). More specifically, Figure 5(c) exhibits

MAS's detailed protection strategy from the time dimension: the earlier activation provides vehicles with sufficient time to pose their positions and orientations and move the impact point backward.

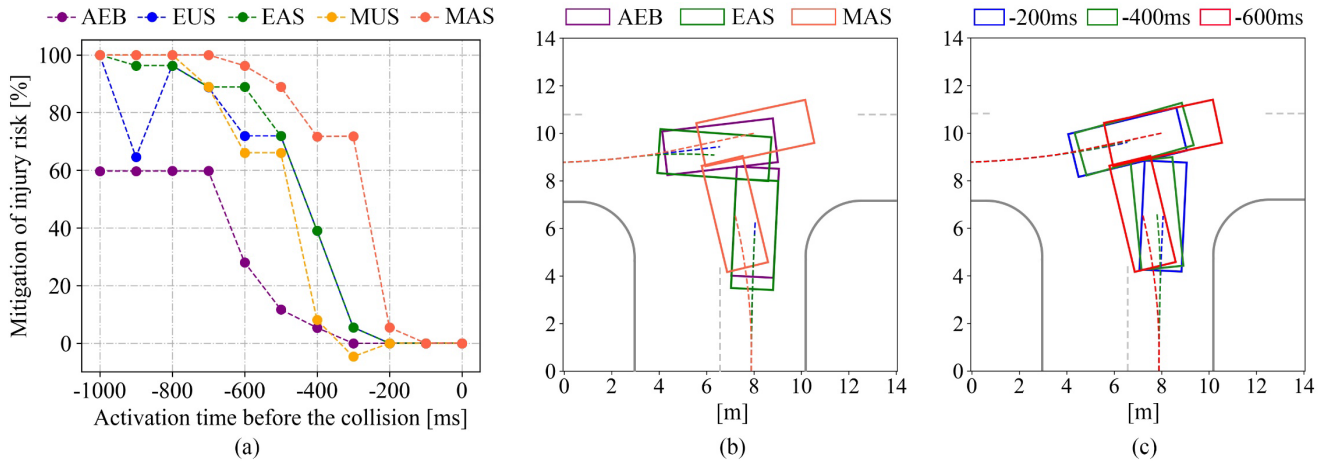


Fig. 5. (a) The mitigation of injury severity in one representative case; (b) the optimized trajectories with different strategies (all strategies activate at -600 ms); (c) the optimized trajectories with different activation times (under MAS).

IV. DISCUSSION

The present results demonstrate that integrating the occupant injury prediction algorithm into the vehicle driving strategy could significantly reduce crash risk and injury severity when confronted with imminent collision scenarios. Specifically, 100% and 37.8% of injury severity were mitigated when the globally optimal strategy (i.e. MAS) was activated at 500 ms and 300 ms before the collision, respectively. All four safety-focused strategies significantly outperformed AEB, demonstrating that the current vehicle occupant protection needs to be further improved. It should be highlighted that the current AEB may even aggravate injuries in some extreme cases as compared to human drivers in the real-world (i.e. negative injury mitigation in Fig. 4). In these cases, human drivers, who are probably experienced, perceived dangers early enough and took an appropriate combination of braking and swerving to better control vehicle dynamics than braking only by AEB. We also found similar phenomena in three safety-focused strategies (i.e. EUS, EAS, MUS) due to the incomplete perception information and the limited controllable objects. By comparison, the MAS manages to reduce injury risk in all situations. This indicates that there may be risks of aggravating injuries when using the locally optimal strategies.

Several limitations should be noted. First, since detailed accident reconstructions take large amounts of manpower and material resources, we only obtained 20 real-world cases. The limited amount might reduce the reliability of statistical analysis and should be further expanded. Second, the CNN-based prediction algorithm is used in both the optimization and injury mitigation assessment, therefore the possible injury prediction error has not been considered. We also assumed that there is no out-of-position displacement of occupants, which might magnify prediction errors. Meanwhile, we have not yet considered the error and time delay of vehicle perception, decision and execution processes. As the injury severity prediction is a critical component of this framework, the effectiveness in a more realistic manner shall be assessed in subsequent studies. Finally, for performing a direct comparison, we largely simplified the complex activation mechanism in real on-vehicle AEB systems, which might have reduced its performance. Further efforts are necessary to produce more accurate and credible injury mitigation results of the proposed safety-focused strategies in imminent collision scenarios.

V. ACKNOWLEDGEMENTS

This work was supported in part by the National Natural Science Foundation of China (51705276, 51675295), the Young Elite Scientist Sponsorship Program by CAST (2018QNRC001) and the National Key R&D Program of China (2017YFE0118400, 2018YFE0192900).

VI. REFERENCES

- [1] Badue, C., et al., *Expert Syst Appl*, 2020.
- [2] Nie, B., et al., *Traffic Inj Prev*, 2016.
- [3] Ishikawa, H., *SAE Transactions*, 1994.
- [4] Bance, I., et al., *IRCOBI*, 2019.
- [5] Bance, I., et al., *Sci China Technol Sci*, 2020.